Effect of Post-weld Heat Treatment on the Mechanical Properties of Supermartensitic Stainless Steel Deposit

Sebastián Zappa, Hernán Svoboda & Estela Surian

Journal of Materials Engineering and Performance

ISSN 1059-9495
Volume 26
Number 2

J. of Materi Eng and Perform (2017)
26:514-521
DOI 10.1007/s11665-016-2467-8

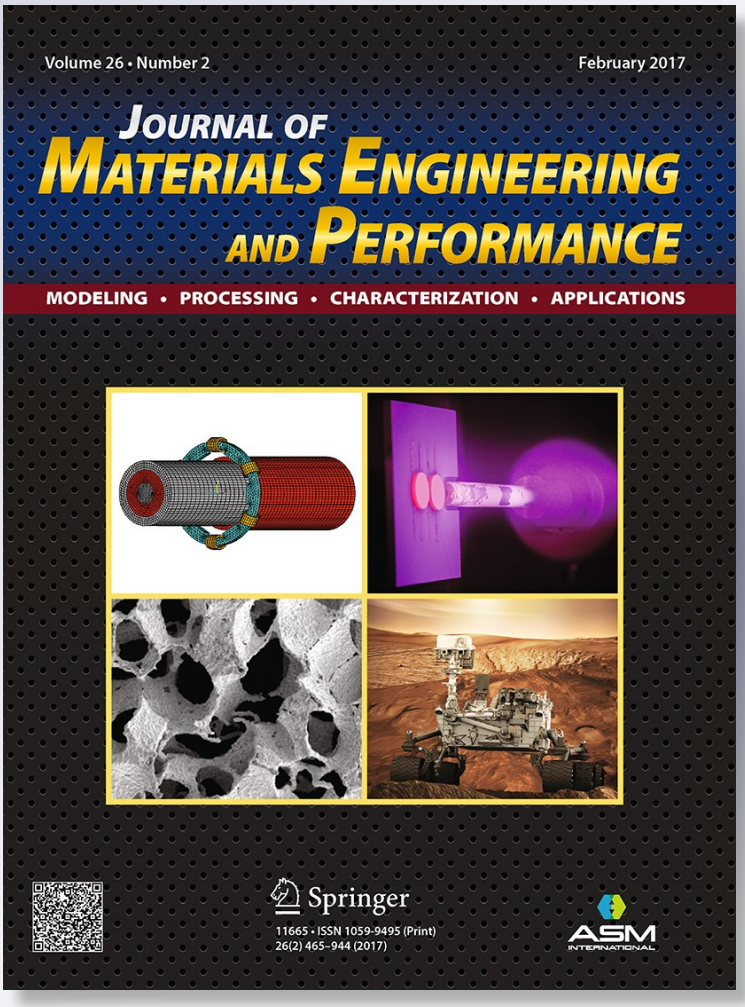

Springer

JMEPEG (2017) 26:514–521
DOI: 10.1007/s11665-016-2467-8

1059-9495/$19.00

Effect of Post-weld Heat Treatment on the Mechanical Properties of Supermartensitic Stainless Steel Deposit

Sebastián Zappa, Hernán Svoboda, and Estela Surian

(Submitted February 24, 2016; in revised form October 19, 2016; published online December 20, 2016)

Supermartensitic stainless steels have good weldability and adequate tensile property, toughness and corrosion resistance. They have been developed as an alternative technology, mainly for oil and gas industries. The final properties of a supermartensitic stainless steel deposit depend on its chemical composition and microstructure: martensite, tempered martensite, ferrite, retained austenite and carbides and/or nitrides. In these steels, the post-weld heat treatments (PWHTs) are usually double tempering ones, to ensure both complete tempering of martensite and high austenite content, to increase toughness and decrease hardness. The aim of this work was to study the effect of post-weld heat treatments (solution treatment with single and double tempering) on the mechanical properties of a supermartensitic stainless steel deposit. An all-weld metal test coupon was welded according to standard ANSI/AWS A5.22-95 using a GMAW supermartensitic stainless steel metal cored wire, under gas shielding. PWHTs were carried out varying the temperature of the first tempering treatment with and without a second tempering one, after solution treatment. All-weld metal chemical composition analysis, metallurgical characterization, hardness and tensile property measurements and Charpy-V tests were carried out. There are several factors which can be affected by the PWHTs, among them austenite content is a significant one. Different austenite contents (0-42%) were found. Microhardness, tensile property and toughness were affected with up to 15% of austenite content, by martensite tempering and carbide precipitation. The second tempering treatment seemed not to have had an important effect on the mechanical properties measured in this work.

Keywords austenite content, post-weld heat treatment, SMSS all-weld metal, tensile property, toughness

1. Introduction

Supermartensitic stainless steels (SMSSs) were developed based on classic martensitic steels (11-14% Cr), reducing C and increasing both Ni and Mo contents (Ref 1, 2). The low C content improves weldability, decreases hardness and increases corrosion resistance; Ni provides a completely martensitic structure, free from delta ferrite; Mo increases corrosion resistance (Ref 1-4). These steels are a lower-cost technological alternative to be applied in hydraulic turbines, valve bodies, high-pressure pipelines, over all in the oil and gas industry and transportation pipes, in land as well as in off-shore platforms, due to their good mechanical properties and corrosion resistance (Ref 5-7).

Gas metal arc welding (GMAW) using SMSS metal cored wires has been recognized as an alternative to weld these materials, and its industrial implementation has been increased in the last times (Ref 2).

As-welded (AW) SMSS deposits present a martensitic structure with some fractions of delta ferrite and retained austenite in low proportions; these facts can compromise ductility, toughness and corrosion resistance (Ref 8, 9).

The PWHs are usually necessary to adjust the final properties of the SMSS welding deposits, based on the microstructure evolution (control of martensite tempering, austenite content, precipitation phenomena, etc.) (Ref 8). The PWHTs are different for each SMSS grade. In AW condition, SMSS deposits show high hardness and low toughness (Ref 4, 9). For these steels, single and double tempering treatments are used to assure the tempering of martensite and to maximize the retained austenite content, producing a decrease in hardness and improving toughness (Ref 2, 10). Solution treatments between 950 and 1050 °C produce homogenization of the chemical composition, as well as the elimination of any delta ferrite (Ref 8, 11). With single and double tempering treatments, it is possible to decrease martensite hardness (Ref 12) and to modify retained austenite contents, depending on their temperature and time (Ref 8, 9, 13).

The austenite content is an important phase in these deposits because it can modify hardness, tensile property, toughness and corrosion resistance. Through the appropriate heat treatments, it is possible to obtain high contents of austenite in the microstructure (Ref 14).

This work is a continuation of a previous paper (Ref 8). Its objective was to study the effect of post-weld heat treatment on hardness, tensile property and Charpy-V toughness of a SMSS all-weld metal obtained using a GMAW metal cored tubular wire. The samples were submitted to solution treatment with

Sebastián Zappa, Faculty of Engineering, National University of Lomas de Zamora, 1832, Lomas de Zamora, Buenos Aires, Argentina; and National Scientific and Technical Research Council, CABA, C1425FQB Buenos Aires, Argentina; **Hernán Svoboda**, National Scientific and Technical Research Council, CABA, C1425FQB Buenos Aires, Argentina; and Faculty of Engineering, University of Buenos Aires, CABA (1063), Buenos Aires, Argentina; and **Estela Surian**, Blanco Encalada 4580, 12 A, CABA, (CP1431), Buenos Aires, Argentina. Contact e-mail: zappasebastian@hotmail.com.

single and double tempering, varying the first tempering temperature. The motivation for this work was to find the condition of post-weld heat treatment that produces greatest toughness.

2. Experimental Procedure

An all-weld metal coupon was welded according to the ANSI/AWS A5.22-95 standard (Ref 15), using a tubular metal core wire of 1.2 mm diameter with the semiautomatic welding process, under gas shielding. The welding position was flat, and the preheating and interpass temperatures were 100 °C. Gas flow was 18 L/min, and stick-out was 20 mm. After been welded, the coupon was x-rayed (XR) following ANSI B31.3-96 standard (Ref 16). The base metal employed was a CMn steel buttered with the consumable to be tested, according to Ref 15. The welding parameters used are presented in Table 1. The parameter values are the average of those monitored during the welding of each bead; the heat input is the result of the average of those of each bead.

On cross sections of the all-weld metal coupon, chemical composition determination, metallographic analysis and Vickers microhardness H_{V1} measurements were performed, in the circle shown in Fig. 1.

Chemical composition was carried out by optical emission spectrometry (OES), except C, O, N and S contents which were analyzed by combustion method. Transversal tensile strength test samples were machined according to ASTM E8:2004 standard (Ref 17) and Charpy-V specimens to ASTM E23:2005 (Ref 18) standard, as indicated in Fig. 2. The strain rate used for the tension test was 0.083 1/min. The particularity of these samples is that both the calibrated zone of the tensile property specimen and the Charpy-V sample notch were located in the all-weld metal zone. On these samples, two series of PWHTs [selected according to the literature (Ref 1, 9, 19)], were performed. Table 2 shows the sample identification and the heat treatments carried out.

In all cases, after solution treatment during 60 min, cooling was made in water; after first and second tempering treatments, cooling was in air. The microstructural characterization was performed by light microscopy (LM), scanning electron microscopy (SEM) and x-ray diffraction (XRD). Samples were mechanically polished and etched before observation by LM and SEM. Vilella's reagent (95 mL ethanol, 5 mL HCl, 1 g picric acid) was used to reveal the microstructure at LM and SEM. XRD was performed with Cu radiation (λ = 1.5408 Å) within a scan range of 30°-90° (2θ) with a step size of 0.05° and with a scanning rate of 0.5° min^{-1}. The retained austenite contents were determined using the peak comparison method from the XRD patterns (Ref 20). Ferrite contents, in AW condition, were measured following standard ASTM E562-99 (Ref 21), by quantitative metallography. Tensile and impact Charpy-V samples were tested in the AW and PWHT conditions at room temperature.

3. Results and Discussion

The XR test of the coupon showed a low level of defects. In Fig. 1, a macrograph of a transversal cut of the welded coupon can be seen, showing the base metal, the buttering and the all-weld metal zone; on this last area, all the tests were carried out. Table 3 shows the chemical composition determined in wt.%, except those of C, O and N which are expressed in ppm.

The all-weld metal chemical composition obtained was consistent with the nominal values for this alloy. C, Si, Mo and N contents were slightly higher and Mn, Cr, Ni and Cu slightly lower than those informed by the consumable producer (Ref 22, 23).

In SMSS deposits, to reach a good toughness and appropriate hardness it is necessary to have low C, N, O and S contents (Ref 24, 25). C, which controls both martensite hardness and toughness, is the more influent element on M_S temperature (Ref 26). Among other things, carbide precipitation influences corrosion resistance and hydrogen embrittlement (Ref 26). Additionally, N and Mo influence the carbide and carbonitride precipitation sequence (Ref 27). Regarding O content, it was higher than 300 ppm, limit from which the absorbed energy in Charpy-V test abruptly falls, according to the literature (Ref 22).

Figure 3 presents the XRD diffraction patterns for the different heat treatment conditions. Table 4 shows the retained austenite contents and Fig. 4 the evolution of the austenite content with the heat treatment.

Through LM and SEM and Fig. 3, it was possible to observe that the microstructure in AW condition was formed by a martensitic matrix with low contents of both ferrite and retained austenite, according to previous works of the authors (Ref 8, 9). Also, it can be observed that the microstructure obtained after solution treatment, was completely martensitic, without ferrite or retained austenite. With the first tempering performed from 580 to 680 °C, the austenite content increased up to a maximum (14%) for sample 620ST and then decreased.

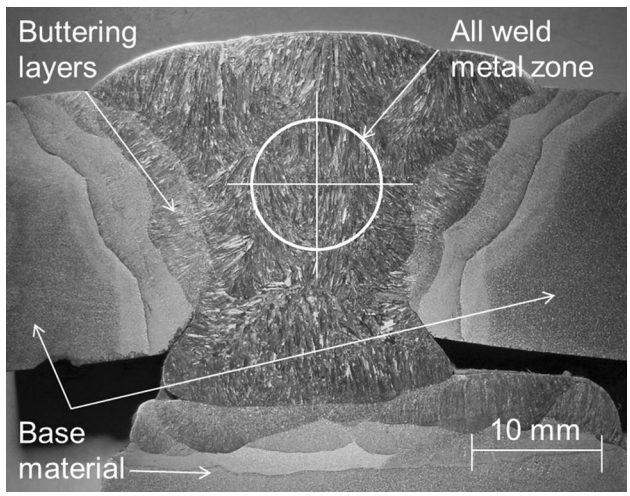

Fig. 1 Transversal cut of all-weld metal coupon

Table 1 Welding parameters

Shielding gas	Tension, V	Current, A	Welding speed, mm/s	Wire speed, mm/s	Heat input, kJ/mm
Ar + 2% CO_2	29	295	6	9	1.43

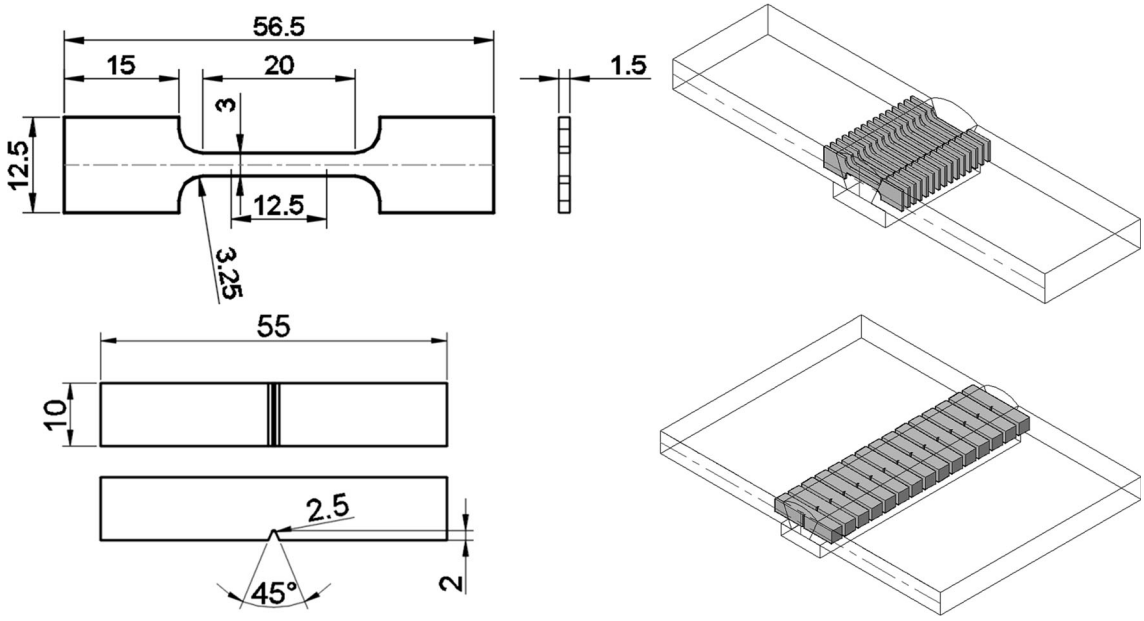

Fig. 2 Transversal tensile strength and Charpy-V test samples (all dimensions are in mm)

Table 2 Sample identification according to the thermal cycle applied

Identification	Solution treatment	First tempering	Second tempering
AW	…	…	…
1000S	1000 °C, 60 min	…	…
580ST	1000 °C, 60 min	580 °C, 15 min	…
600ST	1000 °C, 60 min	600 °C, 15 min	…
620ST	1000 °C, 60 min	620 °C, 15 min	…
640ST	1000 °C, 60 min	640 °C, 15 min	…
660ST	1000 °C, 60 min	660 °C, 15 min	…
680ST	1000 °C, 60 min	680 °C, 15 min	…
580DT	1000 °C, 60 min	580 °C, 15 min	600 °C, 15 min
600DT	1000 °C, 60 min	600 °C, 15 min	600 °C, 15 min
620DT	1000 °C, 60 min	620 °C, 15 min	600 °C, 15 min
640DT	1000 °C, 60 min	640 °C, 15 min	600 °C, 15 min
660DT	1000 °C, 60 min	660 °C, 15 min	600 °C, 15 min
680DT	1000 °C, 60 min	680 °C, 15 min	600 °C, 15 min

S solubilizing, *ST* single tempering, *DT* double tempering

Table 3 All-weld metal chemical composition in wt.%: first line, measured values; second line, batch values informed by the consumable producer

C	Mn	Si	S	P	Cr	Ni	Mo	Cu	V	O	N
150	1.7	0.44	0.015	0.015	11.9	6.11	2.69	0.46	0.09	490	110
< 100	1.8	0.40	…	…	12.5	6.70	2.50	0.50	…	…	< 100

According to Gooch et al. (Ref 28), in high Ni content alloys, the temperature A_{C1} can be around 550 °C.

A_{C1} of the deposit was determined using the following formula:

$$A_{C1}(^{\circ}\mathrm{C}) = 850 - 1500(\mathrm{C}+\mathrm{N}) - 50\mathrm{Ni} - 25\mathrm{Mn} + 25\mathrm{Si} + 25\mathrm{Mo} + 20(\mathrm{Cr}\text{-}10) = 575\,^{\circ}\mathrm{C}$$

At 580 °C, partial transformation to austenite is produced.

At this temperature, the kinetic of precipitation of carbides is very slow and it is normal that austenite forms (Ref 28). In this way, through a diffusional mechanism, the austenite produced during the tempering is enriched in elements such as N, C and Ni (Ref 28, 29). This enrichment will determine the stability of austenite formed during the treatment.

If tempering is carried out at temperatures slightly above A_{C1}, the enriched austenite will be stable at room temperature (Ref 28, 29). On the other hand, if the treatment is performed at temperatures well above or well below A_{C1}, the austenite will lose chemical enrichment and, consequently, its stability: It will be transformed to fresh martensite during cooling (Ref 28).

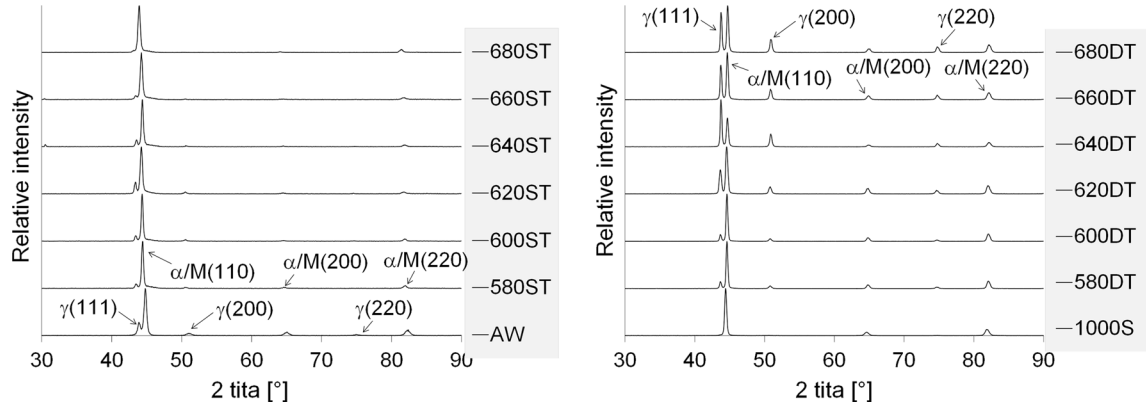

Fig. 3 XRD diffraction patterns for the different heat treatment conditions

Table 4 Retained austenite content

Sample	AW	1000 S	580 ST	600 ST	620 ST	640 ST	660 ST	680 ST	580 DT	600 DT	620 DT	640 DT	660 DT	680 DT
Austenite content (%)	18	0	7	9	14	9	6	3	10	22	25	42	33	30

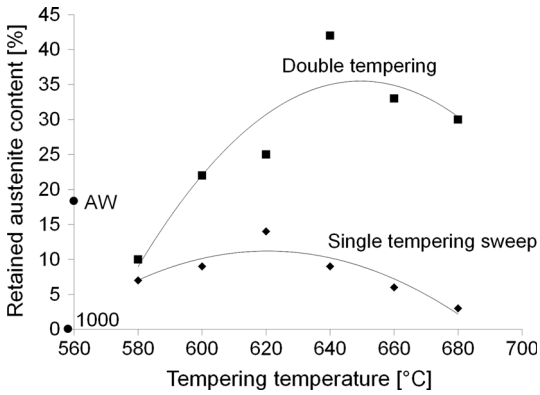

Fig. 4 Evolution of the retained austenite content

Highest contents of austenite will be obtained with tempering temperatures 40-50 °C above A_{C1}, according to Gooch et al. (Ref 28).

In agreement with other authors (Ref 30, 31), the quantity of retained austenite increases with the tempering treatment temperature. Therefore, for a high treatment temperature (above A_{C1}) high austenite content is produced. However, the concentration of austenite stabilizing elements, such as C and Ni, gradually decreases, decreasing the stability of the austenite during the PWHT (Ref 30, 31). The retained austenite behavior found in this work could be associated with the chemical stability generated during the thermal cycles, as it was described.

In these conditions of heat treatment (S + T), it was obtained:

- tempered martensite;
- precipitates (carbides or nitrides);
- austenite: increased up to 620 °C and then decreased;
- fresh martensite: in constant growing;

Double tempering samples showed the same behavior than those with only a tempering. Austenite content increased up to a maximum (42%), in sample 640DT, and then decreased. The microstructure was tempered martensite with high retained austenite content without delta ferrite.

The mechanism, through which the austenite content increased with the double tempering treatment, can be explained by the thermal instability of the austenite generated with the first tempering (Ref 1, 32, 33).

Austenite stability at room temperature is associated with two phenomena:

(a) a chemical factor (single tempering case)
(b) a structural factor related to a high dislocation density in the substructure.

This means that the austenite stability influences not only the solute segregations but also the dislocation density (Ref 33).

After the solution treatment, with the first tempering, the austenite formed during heating increases in an important quantity but it is not enough stable from the thermal point of view. That is to say that this austenite transforms partially to martensite with the posterior cooling (Ref 33).

In this last condition, the microstructure is composed by tempered martensite, fresh martensite with the original morphology of the retained austenite from which it comes, and retained austenite.

Now then, during the second tempering at 600 °C, a higher quantity of austenite laths is formed from the new fresh martensite recently created. It is assumed that austenite is formed through a shear cutting mechanism (shearing in the crystalline net due to a cooperative movement of atoms through short distances) in martensitic matrix regions enriched in segregated austenitizing elements. On the other hand, fresh martensite decomposes to tempered martensite. In this way, as a result of the double tempering, it is produced an increment of austenite with a more uniform distribution (Ref 1, 33), inside the completely tempered martensitic matrix.

As it was previously mentioned, AW microstructure was constituted by martensite with low fractions of ferrite (around 9%) and retained austenite (18%). Solution treatment at 1000 °C × 60 min followed by cooling in water was affective to both homogenize chemical composition and dissolve ferrite. After cooling under these conditions, ferrite was not observed by LM or SEM, and no austenite was identified by XRD, assuming a microstructure constituted by 100% martensite.

Regarding the tempering treatments and in a general way, it can be mentioned that there were not found marked differences at LM and SEM, when comparing the samples treated with the same first tempering temperature, with and without the second tempering treatment.

As the first tempering temperature increased, it was observed in the microstructure a coarse precipitation in grain borders.

Figure 5 presents SEM images of the microstructure of samples 580ST, 580DT, 640ST, 640DT, 680ST and 680DT.

In these images it can be noticed a second phase in the interior of the grains, as it is mentioned in the literature (Ref 34), for this type of materials in similar conditions. According to Divya et al. (Ref 34), the microstructure will consist of a martensitic matrix with second aligned phases with width below submicroscopic levels.

In agreement with what is observed in Fig. 5, the submicroscopic second phase content grew in the same way the retained austenite content did. Other authors (Ref 30) indicate that the microstructure consists of martensite and retained austenite with particles similar to those found in this work. In accordance with this discussion, the submicroscopic second phases shown in the SEM images of Fig. 6 could be retained austenite; this is for the sample with the highest austenite content which was analyzed with different magnification. The width of the particles could be in the order of 100-200 nanometers.

According to the literature (Ref 30), at the tempering temperatures used in this work, carbide precipitates are formed. $M_{23}C_6$-type precipitates form and grow from 500 °C up to A_{C1} temperature, and they can produce secondary hardening. Other authors (Ref 31) inform that at tempering temperature of 650 °C, a fine precipitation of the same type of carbides is produced inside the martensitic matrix, generating tempered martensite. In this sense, at 600 °C of tempering temperature $Cr_{23}C_6$ and Cr_7C_3 carbides, rich in Cr, are formed in the primary austenite grain borders (Ref 14). On the other hand, it is informed (Ref 35) that in SMSS welding deposits, at tempering temperature higher than 550 °C, it is promoted the precipitation of 20 nm carbonitrides along the border of the martensite laths. When the tempering temperature is higher than 600 °C, the quantity and size of the carbonitrides increase. Finally, with XRD (Ref 33), identifies M_7C_3- and $M_{23}C_6$-type carbides with high N and Mo contents for both simple and double tempering treatments. N promotes M_2(C, N) carbonitrides formation at the expenses of M_7C_3 and $M_{23}C_6$ (Ref 33).

In Fig. 7, high-magnification SEM images are presented. In Fig. 7(a) (580ST sample), it can be observed a fine precipitation on martensite laths associated with its tempering.

In Fig. 7(b) (580DT sample), the same precipitation appeared indicating that the second tempering (at 600 °C) did not alter the precipitation produced by the first one; there was only an increase in the austenite content.

The size of these fine precipitates was in the order of 50-100 nm. They could be associated with carbonitrides as it was previously described.

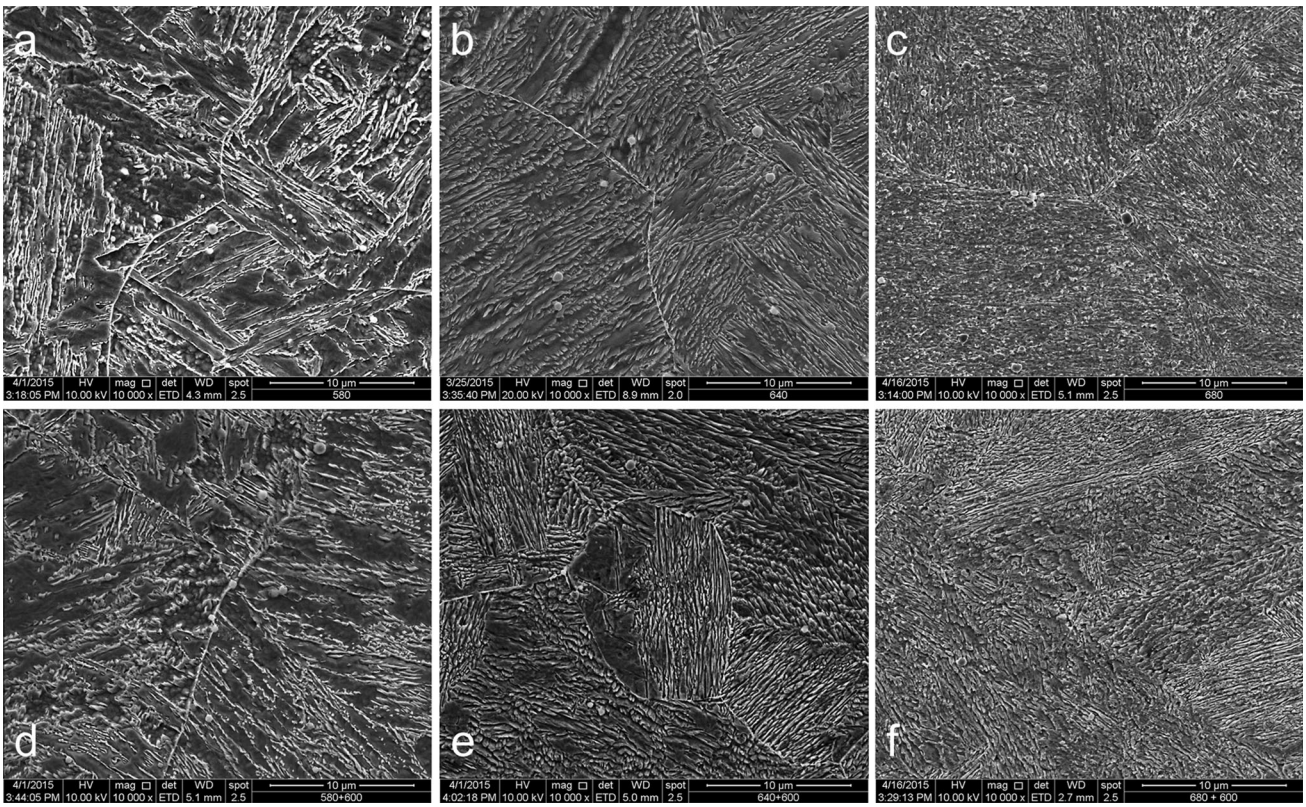

Fig. 5 Microstructures obtained with SEM. (a) 580ST, (b) 640ST, (c) 680ST, (d) 580DT, (e) 640DT, (f) 680DT

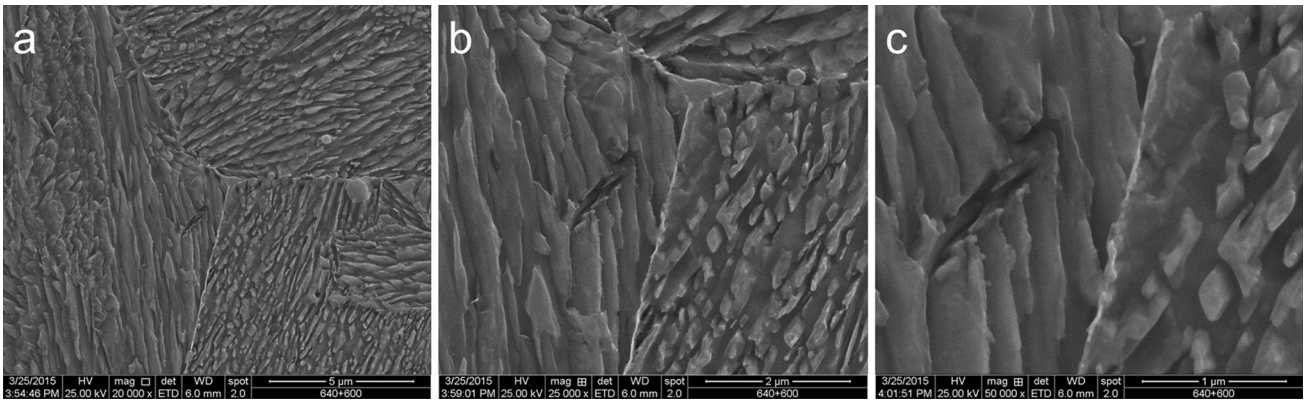

Fig. 6 Retained austenite in 640DT specimens. (a) ×20,000, (b) ×25,000, (c) ×50,000

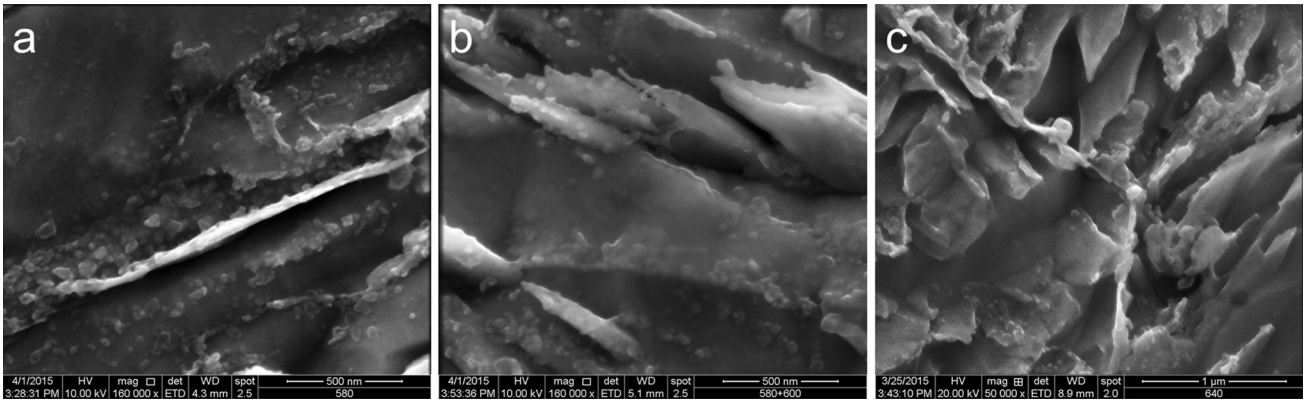

Fig. 7 Fines precipitated. (a) 580ST ×160,000, (b) 580DT a ×160,000, (c) 640ST a ×50,000, (d) 680 a ×80,000

In Fig. 7(c) (640ST sample), there was a coarser precipitation in the grain border which could be related to carbides of the types M_7C_3 and $M_{23}C_6$. Similar results were found for the rest of the samples.

The AW sample (which microstructure was formed by martensite and small fractions of both ferrite and retained austenite) showed hardness of 341 H_{V1}, yield strength of 950 MPa, tensile strength of 1144 MPa and Charpy-V absorbed energy of 32 J.

With the solution treatment, followed by cooling in water (1000S sample) hardness and tensile property decreased and toughness increased. These differences could be associated with the elimination of ferrite and homogenization of both chemical composition and microstructure, as the microstructure was constituted by fresh martensite.

Figure 8 presents representative stress-strain plots from the tension test.

Figure 9(a) and (b) shows the effect of the different thermal treatments on mechanical properties.

With the increment of the first tempering temperature, hardness and tensile property reached minimum values for 620 °C treatment temperature. Above this temperature, the mentioned properties increased again. Toughness and elongation showed the opposite behavior, reaching both properties maximum values for 620 °C of treatment temperature.

The explanation of single tempering treatments results could be associated with the tempering of martensite and the austenite content observed in the microstructure by XRD. The content of this last face, as a function of the tempering temperature,

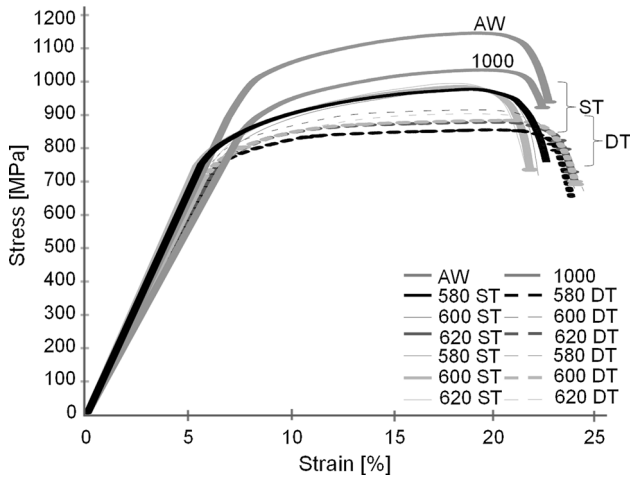

Fig. 8 Representative stress-strain plots from the tension test

showed maximum values when minimum hardness and maximum ductility were measured (Ref 14) (Fig. 9a and b).

In this sense, according to Fig. 3, the austenite content decreased for tempering temperature higher than 620 °C generating fresh martensite (Ref 8, 9). The fresh martensite content grew from 620 to 680 °C of tempering temperature increasing both hardness and tensile property and decreasing toughness.

Similar behavior was found for samples with double tempering: when first tempering temperature increased tensile

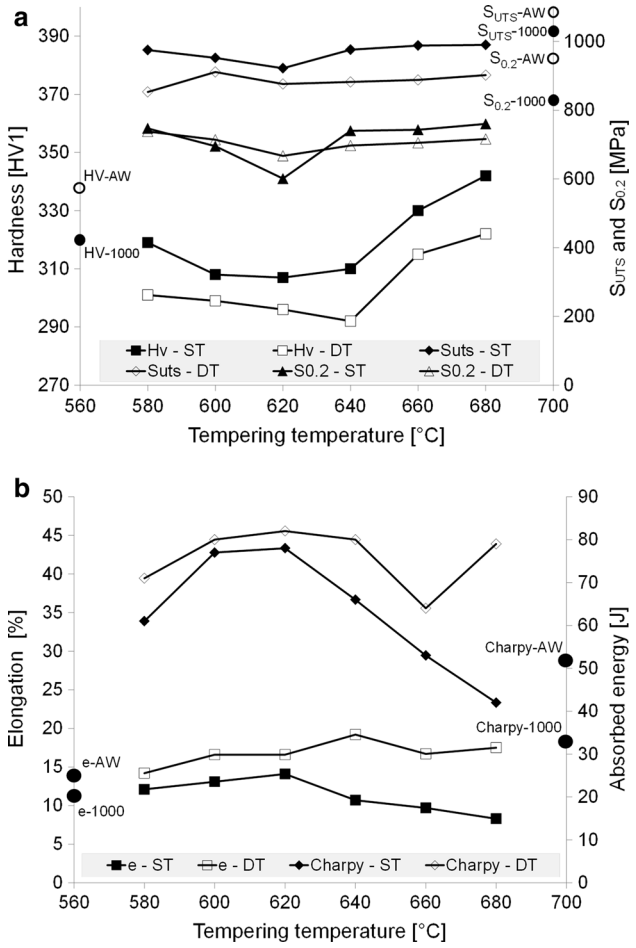

Fig. 9 (a) Relationship between tempering temperature and hardness, tensile strength/yield stress, (b) relationship between tempering temperature and elongation/absorbed energy

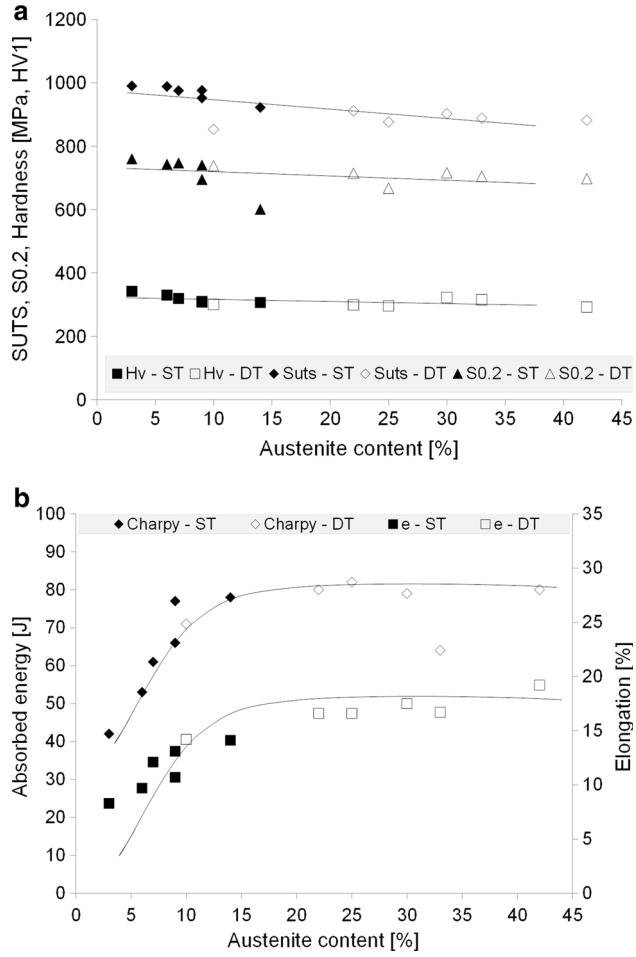

Fig. 10 (a) Relationship between austenite content and hardness, tensile strength/yield stress, (b) relationship between austenite content and elongation/absorbed energy

and yield strengths as well as hardness decreased up to 620-640 °C, fundamentally due to the tempering of martensite and the higher retained austenite content, facts which generated a strong structural softening.

For samples 620DT and 640DT the minimal values of hardness and tensile property were achieved. With the successive increment of first tempering temperature, from 660 °C, these properties increased.

Figure 10(a) and (b) show the relationship among austenite content and hardness, tensile property and Charpy-V impact toughness measured at room temperature, for the different tempering temperatures, in which it can be observed the effect of retained austenite content on the studied properties.

According to Fig. 10(a) and (b), the highest variations in the mechanical properties were achieved up to a 15% of austenite content. For higher values of austenite content, in general terms, mechanical properties were approximately constant.

4. Conclusions

The AW sample presented a microstructure constituted by a martensitic matrix with fractions of ferrite and retained austenite.

The thermal cycles applied to SMSS welding deposits showed that:

With the solution treatment at 1000 °C and cooling in water, the microstructure was completely fresh martensitic.

With the single tempering (varying its temperature between 580 and 680 °C), there was a maximum of austenite content (14%) for 620 °C. In this condition there was a slightly decrease in both hardness and tensile property but a significant increase in toughness and ductility.

With double tempering treatments, the austenite content showed the same behavior than with only one, being the values higher than those obtained with single tempering, comparing the samples treated at the same first tempering temperature. Austenite content increased up to 42% at 640 + 600 °C. Again, hardness and tensile property decreased and both toughness and ductility increased with the increase in austenite content.

Second tempering generated an increment in the austenite content and slightly variations in the mechanical properties.

As a general conclusion, it seems not to be justifiable to perform the second tempering treatment as the improvement in toughness here measured was very little, in the conditions and materials here studied.

Acknowledgments

The authors wish to express their gratitude to ESAB, Sweden, for the donation of the consumable and performing LECO chemical analysis, to CONARCO-ESAB Argentina for performing chemical analysis, to Air Liquide Argentina for donating gases for welding, to the Latin American Welding Foundation, Argentina, for facilities for welding and mechanical testing, to the Scanning Electron Microscopy Laboratory of Inti-Mechanics, Argentina, for facilities for SEM analysis and to APUEMFI, Argentina, for financial support.

References

1. P.D. Bilmes, *Role of Austenite in the Mechanical Properties of Soft Martensitic Stainless Steels Weld Metals*, Engineering doctoral thesis, National University of La Plata, 2000, p 147 **(in Spanish)**
2. J.C. Lippold and D.J. Kotecki, *Martensitic Stainless Steel, Welding Metallurgy and Weldability Of Stainless Steels*, 1st ed., Wiley, New York, 2005, p 56–86
3. L. Karlsson, S. Rigdal, G. Sweden, W. Bruins, and M. Goldschmitz, Development of Matching Composition Supermartensitic Stainless Steel Welding Consumables, *Svetsaren*, 1999, **3**, p 3–7
4. P.E. Kvaale and S. Olsen, *Experience with Supermartensitic Stainless Steels in Flowline Applications*, Stainless Steel Word Conference, (The Netherlands), 1999, p 19–26
5. A.W. Marshall and J.C.M. Farrar, *Welding of Ferritic and Martensitic 13% Cr Steel*, International Institute of Welding (France), IIW Doc IX-H-422-98, 1998, p 1–18
6. J.C. Farrar and A.W. Marshall, *Supermartensitic Stainless Steel—Overview and Weldability*, International Institute of Welding (France), IIW Doc IX-H 423-98, 1998, p 1–3
7. A.W. Marshall and J.C.M. Farrar, Welding of ferritic and martensitic 11–14% Cr steels, *Weld. World*, 2001, **45**(5), p 32–55
8. S. Zappa, H. Svoboda, M. Ramini, E. Surian, and L. de Vedia, Improving Supermartensitic Stainless Steel Weld Metal Toughness, *Weld. J.*, 2012, **91**(3), p 83–90
9. S. Zappa, H. Sovoboda, M. Ramini, E. Surian, and L. de Vedia, Effect of Post-weld Heat Treatment on the Properties of a Supermartensitic Stainless Steel Deposited with Tubular Metal-Cored Wire, *Soldag. Insp.*, 2007, **12**(2), p 115–123 **(in Spanish)**
10. P.D. Bilmes, C.L. Llorente, and M. Solari, *Effect of Postweld Heat Treatment on the Microstructure and Mechanical Behavior of 13Cr–4NiMoL and 13Cr–6NiMoL Weld Metals*, The 18th ASM Heat Treating Society Conference and Exposition (Chicago, USA), 1998, p. 454–466
11. P.D. Bilmes, C. Llorente, J. Desimoni, R. Mercader, and M. Solari, *Microstructures and properties of weld metals FCAW soft martensitic stainless steels, II Encuentro de Ingenieria de Materiales*, September (La Habana, Cuba), 1998 **(in Spanish)**
12. J. Lippold and B. Alexandrov, *Phase Transformations During Welding and Postweld Heat Treatment of 12Cr–6.5Ni–2.5Mo Supermartensitic Stainless Steel*, Stainless Steel World 2004, October (Houston, USA), 2004
13. O.M. Akselsen, G. Rorvik, P.E. Kvaale, and C. Van-der-Eijk, Microstructure–Property Relationships in HAZ of New 13% Cr Martensitic Stainless Steel, *Weld. J.*, 2004, **83**(5), p 160–167
14. B. Akhavan, F. Ashrafizadeh, and A.M. Hassanli, Influence of Retained Austenite on the Mechanical Properties of Low Carbon Martensitic Stainless Steel Castings, *ISIJ Int.*, 2011, **51**(3), p 471–475
15. *"Specification for Stainless Steel Electrodes for Flux Cored Arc Welding and Stainless Steel Flux Cored Rods for Gas Tungsten Arc Welding"*, A5.22, AWS Standards, American Welding Society, 1995
16. *"Chemical Plant and Petroleum Refinery Piping"*, B31.3, ANSI Standard, American National Standards Institute, 1996
17. *"Standard Test Methods for Tension Testing of Metallic Materials"*, E8, ASTM Standards, American Society for Testing Materials, 2004
18. *"Standard Test Methods for Notched Bar Impact Testing of Metallic Materials"*, E23, ASTM Standards, American Society for Testing Materials, 2005
19. P.D. Bilmes, C. Llorente, J. Desimoni, and R. Mercader, *Microstructure and Properties of Soft Martensitic Stainless Steel Weld Metals*, 2do Congresso Internacional de Tecnología Metalúrgica e de Materiais (Sao Paulo, Brasil), 1997
20. B.D. Cullity and S.R. Stock, Quantitative Phase Analysis, *Elements of X-Ray Diffraction*, 3rd Edition Prentice-Hall, Upper Saddle River, 2001, p 351–354
21. *"Standard Test Method for Determining Volume Fraction by Systematic Manual Point Count"*, E562, ASTM Standard, American Society for Testing Materials, 1999
22. L. Karlsson, W. Bruins, C. Gillenius, S. Rigdal, and M. Goldschmitz, *Matching Composition Supermartensitic Stainless Steel Welding Consumables*, Supermartensitic Stainless Steels '99 (Brussels, Belgium), 1999
23. Technical Sheet OK Tubrod, 15-55 ESAB, 2004
24. L. Karlsson, S. Rigdal, J. Van-der-Broek, M. Goldschmitz, and R. Pedersen, Welding of Supermartensitic Stainless Steels, *Recent Dev. Appl. Exp. Svetsaren*, 2002, **2**, p 15–22
25. L. Karlsson, S. Rigdal, A. Dhooge, E. Deleu, M. Goldschmitz, and J. Van-der-Broek, *Mechanical Properties and Ageing Response of Supermartensitic Weld Metals*, Stainless Steel World Conference (The Hague, The Netherlands), 2001
26. J.-Y. Park and Y.-S. Park, The Effects of Heat-Treatment Parameters on Corrosion Resistance and Phase Transformation of 14Cr–3Mo Martensitic Stainless Steel, *Mater. Sci. Eng. A*, 2007, **449–451**, p 1131–1134
27. F.B. Pickering, *Physical Metallurgy and the Design of Steels*, Applied Science, London, 1978
28. T.G. Gooch, P. Woollin, and A.G. Haynes, *Welding Metallurgy of Low Carbon 13% Chromium Martensitic Steels*, Supermartensitic Stainless Steel '99 (Brussels, Belgium), 1999
29. H. Folkhard, *Welding Metallurgy of Stainless Steels*, Springer, New York, 1998
30. D. Zou, Y. Han, W. Zhang, and X. Fang, Influence of Tempering Process on Mechanical Properties of 00Cr13Ni4Mo Supermartensitic Stainless Steel, *J. Iron Steel Res. Int.*, 2010, **8**(17), p 50–54
31. Y. Liu, D. Ye, Q. Yong, and W. Jiang, Effect of Heat Treatment on Microstructure and Property of Cr13 Super Martensitic Stainless Steel, *J. Iron Steel Res. Int.*, 2011, **18**(11), p 60–66
32. S. Zappa, H. Svoboda, and E. Surian, Effects of Welding Procedure on Corrosion Resistance and Hydrogen Embrittlement of Supermartensitic Stainless Steel, *J. Iron Steel Res. Int.*, 2012, **20**(12), p 124–132
33. P.D. Bilmes, M. Solari, and C. Llorente, Characteristics and Effects of Austenite Resulting from Tempering of 13Cr–NiMo Martensitic Steel Weld Metals, *Mater. Charact.*, 2001, **46**(4), p 285–296
34. M. Divya, C.R. Das, V. Ramasubbu, S.K. Albert, and A.K. Bhaduri, Improving 410NiMo Weld Metal Toughness by PWHT, *J. Mater. Process. Technol.*, 2011, **211**(12), p 2032–2038
35. X.P. Ma, L.J. Wang, C.M. Liu, and S.V. Subramanian, Microstructure and Properties of 13Cr5Ni1Mo0.025Nb0.09V0.06N Super Martensitic Stainless Steel, *Mater. Sci. Eng. A*, 2012, **539**, p 271–279